

# Spin fluctuations in the skutterudite compound $\text{LaFe}_4\text{Sb}_{12}$

R. Viennois<sup>1</sup>, S. Charar<sup>1</sup>, D. Ravot<sup>2</sup>, P. Haen<sup>3</sup>, A. Mauger<sup>4,a</sup>, A. Bentien<sup>5</sup>, S. Paschen<sup>5</sup>, and F. Steglich<sup>5</sup>

<sup>1</sup> Groupe d'Étude des Semiconducteurs<sup>b</sup>, Université de Montpellier II, pl. Eugène Bataillon, 34095 Montpellier Cedex, France

<sup>2</sup> Laboratoire de Physicochimie de la Matière Condensée<sup>b</sup>, Université de Montpellier II, pl. Eugène Bataillon, 34095 Montpellier Cedex, France

<sup>3</sup> Centre de Recherche des Basses températures, CNRS, 25 Avenue des Martyrs, BP 166, 38042 Grenoble, France

<sup>4</sup> Fédération de Recherche Matière et Systèmes Complexes<sup>b</sup>, 140 rue de Lourmel, 75015 Paris, France

<sup>5</sup> Max Planck Institut für Chemische Physik fester Stoffe, Nothnitzer Str. 40, 01187 Dresden, Germany

Received 21 January 2005 / Received in final form 25 April 2005

Published online 11 August 2005 – © EDP Sciences, Società Italiana di Fisica, Springer-Verlag 2005

**Abstract.** We report transport, magnetic and thermodynamic properties of the skutterudite compound  $\text{LaFe}_4\text{Sb}_{12}$ . The basic features are a large magnetic susceptibility  $\chi(T)$ , and large electronic coefficient  $\gamma$  of the heat capacity. In particular, a  $T^{1.35}$ ,  $T^{1.7}$ , and  $T^{-2/3}$  temperature dependence of the magnetic susceptibility  $\chi(T)$ , resistivity  $\rho(T)$ , and Grüneisen parameter  $\Gamma(T)$ , respectively, is found at low temperature. An overall understanding of these physical properties is achieved, assuming that  $\text{LaFe}_4\text{Sb}_{12}$  is a non-Fermi liquid system close to a ferromagnetic quantum critical point, with a spin fluctuation temperature  $T_{sf} = 50 \pm 15$  K.

**PACS.** 72.80.Ga Transition-metal compounds – 75.20.En Metals and alloys – 75.40.Cx Static properties (order parameter, static susceptibility, heat capacities, critical exponents, etc.)

## 1 Introduction

For almost one decade, filled skutterudites  $\text{RM}_4\text{X}_{12}$  have been the subject of extensive studies due to their potential application as thermoelements and outstanding physical properties (for a review, see [1]). In the generic formula, R is a rare earth, M is a transition element: M = Fe, Co, ... and X = P, As or Sb. Among them, skutterudites based on M = Fe show outstanding features. Some order magnetically, either in a ferromagnetic state ( $\text{NdFe}_4\text{Sb}_{12}$  [2]), in a ferro or ferrimagnetic state ( $\text{EuFe}_4\text{Sb}_{12}$  [3,4]) or in an antiferromagnetic state ( $\text{PrFe}_4\text{Sb}_{12}$  [5]). Other show no magnetic ordering down to low temperatures as a result of a coherent Kondo ground state ( $\text{CeFe}_4\text{Sb}_{12}$  [6,7]) or of a mixed valence state of the rare earth ( $\text{YbFe}_4\text{Sb}_{12}$  [8]). Some are moderately heavy fermion systems ( $\text{CeFe}_4\text{Sb}_{12}$  [6,7]) other are heavy fermion systems ( $\text{YbFe}_4\text{Sb}_{12}$  [9]), or even extraordinary heavy fermion systems ( $\text{PrFe}_4\text{P}_{12}$  [10,11]), and all are strongly correlated fermion systems [12].

Another outstanding feature specific to Fe-based filled skutterudites is the importance played by Fe in the physical properties. While the contribution of the transition element to the magnetic susceptibility  $\chi$  is usually negligible when  $M \neq \text{Fe}$ , its importance in the particular case

M = Fe is responsible for an excess in the effective magnetic moment deduced from the Curie constant at high temperature, with respect to the effective moment of the rare earth ion alone. The estimation of this contribution has for long remained qualitative, and analyzed in the framework of the ionic model [1–4,12,13]. In this framework, it was assumed i) that both Fe and the rare earth ion contribution to  $\chi(T)$  should follow the Curie-Weiss law at high temperature. ii) that the Curie constants of these two contributions would be additive. iii) that the magnetic contribution of Fe can be analyzed in the framework of localized rather than itinerant magnetism. However, a recent study of  $\text{CeFe}_4\text{Sb}_{12}$  and  $\text{CeFe}_{4-x}\text{Ni}_x\text{Sb}_{12}$  has shown that only hypothesis i) is justified [7,14], while the hypotheses ii) and iii) are violated. Instead, the magnetic contribution of Fe can be estimated from the magnetic susceptibility of  $\text{LaFe}_4\text{Sb}_{12}$ , since the material has almost the same lattice parameter and same carrier concentration, and La is non magnetic [7].  $\text{LaFe}_4\text{Sb}_{12}$  then appears as a key material to distinguish between the physical properties associated to the iron and those associated to the rare earth in Fe-based skutterudites. This is one reason why we found desirable to investigate the physical properties of this compound.

Another reason is that the material is of interest by itself, and it is the only filled skutterudite with nonmagnetic R ion [3,2,14–17], the other R ions being either in a magnetic or in a mixed valence state. The three main

<sup>a</sup> e-mail: [mauger@ccr.jussieu.fr](mailto:mauger@ccr.jussieu.fr)

<sup>b</sup> Laboratoire associé au Centre National de la Recherche Scientifique

characteristics already observed in this compound are: its high magnetic susceptibility  $\chi$  following the Curie-Weiss law [3,14], the change in sign of its thermoelectric power at low temperatures [2], and the large value (between 130 and 190 mJ/moleK<sup>2</sup>) of the electronic coefficient  $\gamma$  of its specific heat capacity [2,15]. This is one order of magnitude smaller than the value ( $\gamma = 1.4$  J/moleK<sup>2</sup>) for PrFe<sub>4</sub>Sb<sub>12</sub> [3,10,18], but still quite comparable to the value met in other Fe-based skutterudites like YbFe<sub>4</sub>Sb<sub>12</sub> where  $\gamma = 140$  mJ/moleK<sup>2</sup> [9], and twice larger than the value ( $\gamma = 63.8$  J/moleK<sup>2</sup>) in CeFe<sub>4</sub>Sb<sub>12</sub> [6], so that LaFe<sub>4</sub>Sb<sub>12</sub> is a moderately heavy fermion system. However, an overall understanding of LaFe<sub>4</sub>Sb<sub>12</sub> is yet missing. Therefore, this paper is doubly focused. First, we report new studies of physical properties of LaFe<sub>4</sub>Sb<sub>12</sub> at very low temperatures. Second, from these new experimental results and some previous studies, we obtain a new insight in the magnetic, heat and electric transport properties of LaFe<sub>4</sub>Sb<sub>12</sub>, we attribute to the non-Fermi liquid (NFL) behavior of highly correlated itinerant d-electrons close to a ferromagnetic instability. To our knowledge, among the filled skutterudite family, NFL effects had been reported so far only in a  $T \ln T$  dependence of the heat capacity and a  $T^{1.65}$  dependence of the resistivity in CeRu<sub>4</sub>Sb<sub>12</sub> [19], and a  $T \ln T$  dependence of the heat capacity of PrFe<sub>4</sub>Sb<sub>12</sub> at the magnetic field  $H \simeq 3$  Teslas which suppresses the magnetic order [2].

The paper is organized as follows. The experimental processes and apparatus are briefly described in Section 2. The magnetic properties including magnetic susceptibility and non linear magnetization are the subject of Section 3. The transport properties are reported in Section 4, while the thermal properties including heat capacity and Grüneisen parameter are reported in Section 5. The results are discussed in Section 6.

## 2 Experimental

The details of the synthesis and characterization are the same as in the case of CeFe<sub>4</sub>Sb<sub>12</sub> [20]. The samples are nearly single phase (at more than 95%) and polycrystalline, with some inclusions of LaSb<sub>2</sub>. The resistivity measurements have been performed between 1.4 K and 300 K using the Van Der Pauw (VDP) method under DC current for  $T > 20$  K, and an AC current for  $T < 20$  K to increase the accuracy of the measurements. The AC Hall effect measurements have been carried out under magnetic fields up to 6 T. The magnetization measurements have been performed using a vibrating sample magnetometer (VSM) from Oxford Instrument in magnetic fields up to 9 T. The heat capacity has been measured between 0.4 and 30 K using the relaxation method in a micro-calorimeter and a PPMS apparatus from Quantum Design. Another parameter investigated in this work is the Grüneisen parameter  $\Gamma$  defined by  $\Gamma = 3\alpha_T B_T V / C_V$  (where  $V$  is the molar volume,  $\alpha_T$  is the isothermal linear expansion coefficient,  $B_T$  is the isothermal bulk modulus and  $C_V$  is the heat capacity). To determine  $\Gamma$ , the thermal expansion

measurement above 4.2 K has been measured with the use of a capacitance method.

## 3 Magnetic properties

The magnetic susceptibility  $\chi(T)$  has been measured for different batches. At  $T > 150$  K, the law:

$$\chi(T) = \chi_p + C/(T + \theta). \quad (1)$$

fits the experimental data. This modified Curie-Weiss law has been used to describe the magnetic susceptibility of other skutterudites such as EuFe<sub>4</sub>Sb<sub>12</sub> [4], although the origin of the temperature-independent component  $\chi_p$  is unknown. In the present case, we have found that  $\chi_p$  depends on the batch and is then extrinsic in nature. We then attribute this term to the Pauli magnetic susceptibility associated to the small amount of secondary phases mentioned in Section 2. We show in Figure 1 the magnetic susceptibility  $\chi(T) - \chi_p$  for two different batches: the first one where  $\chi_p = 0$ , the second one with  $\chi_p = 1.15 \times 10^{-3}$ . The plot of  $(\chi(T) - \chi_p)^{-1}$  as a function of  $T$ , also displayed in Figure 1, illustrates the Curie-Weiss law at  $T > 150$  K. The effective magnetic moment  $\mu_{\text{eff}}$  and Curie Weiss temperature  $\theta$  deduced from this fit are:  $\mu_{\text{eff}} = 2.26\mu_B, \theta = 42$  K for the first batch, and  $\mu_{\text{eff}} = 2.37\mu_B, \theta = 55$  K for the second bath. The result of the fit with the Curie-Weiss law for the first batch is consistent with a preliminary report [14]. In addition, the values of both  $\mu_{\text{eff}}$  and  $\theta$  are consistent in the two batches, at contrast with  $\chi_p$ , and are thus intrinsic properties of LaFe<sub>4</sub>Sb<sub>12</sub>. If the values of the paramagnetic Curie temperature  $\theta$  reported for the two different samples are similar to those reported in a prior work [3] ( $\theta = 51$  K), the effective moment  $\mu_{\text{eff}}$  is different ( $3\mu_B$  in Ref. [3]). This discrepancy might be due to larger amount of secondary phases (around 10%) in their samples. In addition,  $\chi_p$  was not taken into account in this prior work, which affects the value of  $\mu_{\text{eff}}$  in the fitting process. This attribution of the larger value of  $\mu_{\text{eff}}$  to an extrinsic contribution is consistent with the fact that the smaller value of  $\mu_{\text{eff}}$  has been found in our first batch in which the extrinsic contribution  $\chi_p$  vanishes. In addition, no electron paramagnetic resonance (EPR) signal was detected in this batch at room temperature [21]. At low temperature, one might invoke a broadening of the signal due to some impurity spin freezing in random fields to explain the flat EPR spectrum, but this interpretation does not hold at room temperature, where this feature is attributable to the fact that the amount of magnetic impurities is actually very small for this sample. We then consider that the batch 1 sample is of higher quality, and that the effective magnetic moment  $\mu_{\text{eff}} = 2.26\mu_B$  measured on this batch is the best estimate for LaFe<sub>4</sub>Sb<sub>12</sub>. For the same reason, this is the batch we have used to investigate the magnetic, electronic and thermal properties.

Magnetization curves  $M(H)$  illustrated in Figure 2 for batch 1 show a departure from linearity at  $H > 4$  Teslas at low temperature  $T < 50$  K. Orders of magnitude

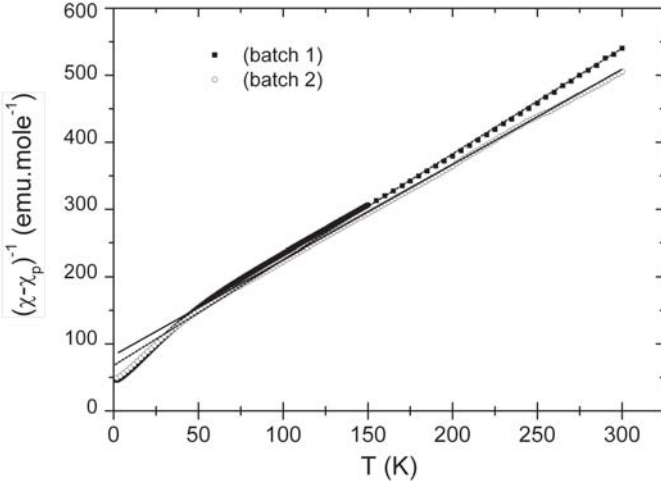


**Fig. 1.** Thermal variation of the inverse of  $\chi(T) - \chi_p$ , where  $\chi(T)$  is the experimental susceptibility, and  $\chi_p$  is constant term attributed to extrinsic effects, different from 0 for batch 2 only (see Eq. (1) in the text). The solid lines correspond to the effective Curie-Weiss law.

smaller departure from linearity is often met in skutterudites [6], including our own samples of CeFe<sub>4</sub>Sb<sub>12</sub> [7], in which case it can be imputed to the existence of magnetic impurities [6,7]. In the present case, however, the origin must be different since the non linear effects are orders of magnitude larger. If we assumed that the magnetization is split between an intrinsic linear contribution, and an extrinsic contribution saturating in a field  $H \simeq 6$  T, the moment at saturation for the impurity contribution would raise to 350 emu/mole at 2 K. This is, however, orders of magnitude too high to be consistent with the magnetic susceptibility data we have just discussed (and with the absence of EPR signal at room temperature above mentioned). It would actually amount to a magnetic impurity concentration the order of 5%, while the starting material has the purity label 3N, 99.9 which corresponds to an impurity concentration the order of few hundreds of ppm only. This non-linear behavior must then be considered as an intrinsic property of the material. We shall discuss the origin of this non-linearity at the end of this section. At this stage, it is sufficient to note that, at the magnetic field (500 G) used in the measurements of the magnetic susceptibility  $\chi(T)$ ,  $M(H)$  is still in the linear (low-field) regime.

The large magnetic susceptibility shows that LaFe<sub>4</sub>Sb<sub>12</sub> is an enhanced paramagnet, so that the material is close to a magnetic instability. In the framework of the Stoner model for band magnetism of transition metals [22], the fact that the material remains paramagnetic at any temperature means that  $U\rho(E_f)$  is smaller but close to 1, where  $U$  is the effective d-d Coulomb correlation potential and  $\rho(E_f)$  the density of Fe d-states at the Fermi energy  $E_f$ . This model, however, involves treating the exchange interaction between itinerant electrons in the d-states of Fe in the mean-field approximation (MFA), while nearness to magnetism implies that spin fluctuations play an important role. Many

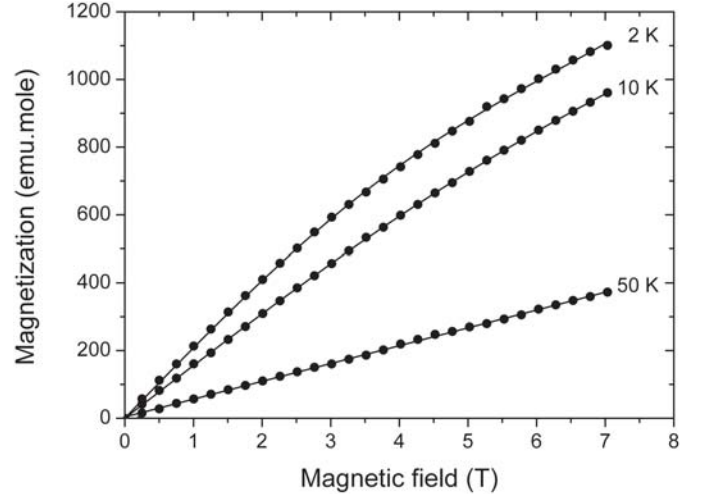


**Fig. 2.** Magnetization curves of batch 1 sample at different temperatures  $T$ . Full symbols correspond to experimental data. The full curves are theoretical fits according to equation (5).

improvements since the pioneering work of Stoner have been made to go beyond the MFA, to include the effect of spin fluctuations [23]. As a result, spin fluctuations do not cause a significant departure of the  $\chi(T)$  from the Curie-Weiss law at high temperature, but the Curie constant and the paramagnetic Curie temperature have to be replaced by effective parameters. In particular, the effective parameter  $\theta$  is no longer related to a magnetic ordering temperature, as the system does not order, but instead, it is related to a spin fluctuation temperature  $T_{sf}$ . Below  $T_{sf}$  the large value of  $U$  (scaled by  $\rho(E_f)$ ) prevents the system from entering the Fermi liquid ground state.

Various spin-fluctuation theories of NFL have been developed [24]. Among them, the self-consistent renormalization model of Moriya and Takimoto [25] has been successful to explain the low-temperature properties of many itinerant d-electron systems. According to this model, the critical part of the magnetic susceptibility scales as  $T^{-\eta}$ , with an exponent  $\eta$  which depends on the dimension  $d$  and the nature of the dominant spin fluctuations (soft mode). For  $d = 3$ ,  $\eta = 4/3$  in the case of ferromagnetic (F) fluctuations and  $\eta = 3/2$  in the case of antiferromagnetic (AF) interactions. Note the scaling applies to the intrinsic part of the magnetic susceptibility  $\chi_i(T) = \chi(T) - \chi_p$ . As we can see in Fig. (1),  $\chi_i(T)$  goes to a finite value  $\chi_i(0)$  at  $T = 0$  rather than diverging. Possible reasons for this behavior observed in various NFL such as doped  $UPt_3$  and CeCu<sub>6-x</sub>(Au, Ag)<sub>x</sub>, has been discussed elsewhere [26,27]. In these cases, the divergent quantity is

$$\left( \frac{1}{\chi_i(T)} - \frac{1}{\chi_i(0)} \right)^{-1} \propto T^{-\eta}. \quad (2)$$

The temperature dependence of  $[1/\chi_i(T) - 1/\chi_i(0)]$  is shown in Figure 3, in a log-log plot, for both batch 1 and batch 2 samples. The power law according to equation (2) is well observed at low temperature. A least square fit of the straight line in this plot gives  $\eta = 1.35$  for both

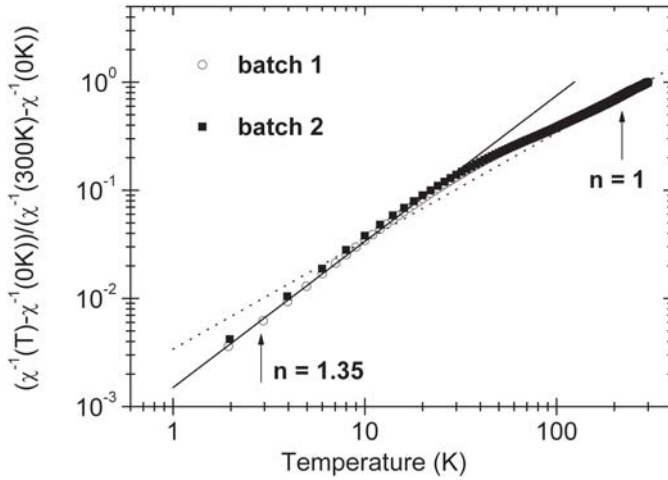


**Fig. 3.** Temperature dependence of  $[1/\chi_i(T) - 1/\chi_i(0)]$  (normalized by its value at room temperature) in a log-log scale. The magnetic susceptibility  $\chi_i(T) = \chi(T) - \chi_p$  is defined in Figure 1. The solid lines correspond to power laws  $T^n$ .  $n = 1$  (dotted line): Curie law at high temperature;  $n = 1.35$  (full line): fit of the data, which illustrates the non-Fermi liquid behavior of  $\text{LaFe}_4\text{Sb}_{12}$  at low temperature.

batches,  $\chi_i^{-1}(T = 0) = 45.2$  and  $48.14$  (emu.mole.Oe) for batch 1 and batch 2 samples, respectively. This value of  $\eta$  is close to  $4/3$  and gives thus evidence that the spin fluctuations are of a ferromagnetic type. If we define the temperature  $\theta^*$  by the relation:

$$\chi_i^{-1}(T) = \chi_i(0)^{-1} [1 + (T/\theta^*)^\eta], \quad (3)$$

we find  $\theta^* = 21.5$  and  $22.3$  K for batch 1 and 2 samples, respectively. Note  $\theta^*$  is also the temperature above which the power-law in equation (2) or equation (3) is no longer valid, which is self-consistent with the meaning of  $\theta^*$  as the temperature below which the system enters the NFL state. We also note that  $\theta \simeq 2\theta^*$ . This gives evidence that  $\theta^*$  is related (same order of magnitude) but different from the spin fluctuation temperatures for reasons outlined earlier in this work: the system shifts continuously in temperature from its low temperature regime ( $T < \theta^*$ ) to its high temperature regime ( $T > \theta$ ). This shift from the  $T^\eta$  to  $T^{-1}$  behavior of  $\chi_i^{-1}(T)$  is also evidenced in Figure 3.

This analysis of the magnetic susceptibility gives an enlightenment on the non-linearity of the magnetization curve at low temperature. Indeed, in a nearly ferromagnetic system, non-linear effects are important, and the magnetization has to be written [30]:

$$M(H) = a_1 H - a_3 H^3 + a_5 H^5. \quad (4)$$

The fit of the intrinsic part of the magnetization ( $M - \chi_p H$ ) by the 5th order polynomial in equation (4) is illustrated in Figure 2, and shows a quantitative fit is obtained up to the highest fields (8 Teslas) investigated. The non-linear effects are measured by the fitting parameters  $a_3$  and  $a_5$ . They vanish at  $T \geq 50$  K and increase upon cooling:  $a_3 = 0.4910^{-12}$ ,  $a_5 = 0.19210^{-22}$  at 10 K, and they reach

the values  $a_3 = 1.6810^{-12}$ ,  $a_5 = 1.27^{-22}$  emu/mole at 2 K. At such magnetic fields where  $\mu_B H$  is negligible with respect to the Fermi energy, such a non linear behavior is not expected in a metal far from a magnetic instability. On another hand, these non-linear parameters  $a_3, a_5, \dots$  diverge at a phase transition. The critical behavior of  $a_3$  has been mainly studied in the particular case of the spin-glass transition, since  $a_1$  remains finite in this particular case [28]. Only recently has the divergence of  $a_3$  also been observed in a paramagnetic metal close to a ferromagnetic quantum critical point [29]. Even if we could not investigate such a divergence in the present work, the increase of both  $a_3, a_5$  upon cooling is clearly stated. The spin glass example shows that the onset of intrinsic non-linearity in the magnetization curve does not imply that the spin fluctuations are necessarily of the ferromagnetic type. In any case, however, this onset is due to large spin fluctuations, and it is then another evidence of the NFL nature of  $\text{LaFe}_4\text{Sb}_{12}$ .

## 4 Transport properties

### 4.1 Resistivity

The resistivity curve  $\rho(T)$  is reported in Figure 4.  $\rho$  is a monotonous increasing function of  $T$ , but shows a negative curvature above an inflection temperature  $T_{\text{inf}} \simeq 65$  K. This is the ‘‘S-shaped’’ behavior, often met in systems dominated by spin fluctuations in a broad class of d-transition metallic compounds and actinide metallic compounds as well (for a review, see [31]). The two main features for these materials with S-shaped resistivity curves is a large resistivity (10–100  $\mu\Omega\text{cm}$ ) at  $T_{\text{inf}}$ , and the fact that  $T_{\text{inf}}$  well compares with the spin fluctuation temperature evaluated from the magnetic susceptibility [31]. The second feature is well verified in our case, since  $\theta \simeq 50$  K, to be compared with  $T_{\text{inf}} \simeq 65$  K. The first feature is also well verified, since the resistivity at room temperature is 450  $\mu\Omega\text{cm}$ . These considerations lead us to make the hypothesis that the diffusion of the free carriers by spin fluctuations is dominant, and we tentatively attribute the saturation effect at high temperature in the  $\rho(T)$  curve to the logarithmic contribution predicted by the spin fluctuation theory [32]. In this framework, we write the contribution of the diffusion by spin fluctuations under the form  $\rho_s(T) = \rho_s(T = T_{\text{inf}}) + b \ln(T/T_{\text{inf}})$ , which holds true from high temperature down to  $T_{\text{inf}}$  where the logarithm term vanishes. In addition, we note that such skutterudites as  $\text{LaOs}_4\text{As}_{12}$  below 3.2 K, or  $\text{LaRu}_4\text{As}_{12}$  below 10.3 K are superconductors [33]. This is a clue that the electron-phonon interaction is important in skutterudites filled with La. This is taken into account by a contribution  $aT$  to the resistivity, which is the phenomenological term standing for the electron-phonon scattering used in the transport properties of metals with strong electron-phonon coupling [34]. The resistivity can thus be written under the form:

$$\rho(T) = \rho_0 + aT + b \ln(T/T_{\text{inf}}) \quad (T \geq T_{\text{inf}}). \quad (5)$$

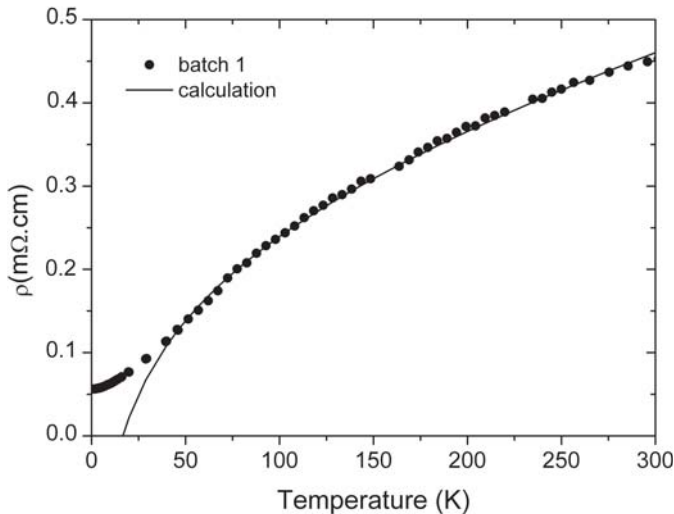


**Fig. 4.** Thermal variation of the resistivity  $\rho(T)$  of the batch 1 sample. The solid line is the theoretical fit according to equation (5) at high temperature.

The term  $\rho_s(T = T_{\text{inf}})$  has been added to the residual resistivity to give the constant term  $\rho_0$  in equation (5). The fit is illustrated in Figure 4, and is actually quite good down to  $T_{\text{inf}}$ . We also note that the addition of a Mott-Jones term of the form  $-a'T^3$  which is successful to fit the resistivity of some transition metal compounds has been found irrelevant to the case of filled skutterudites [4,51] different from  $\text{LaFe}_4\text{Sb}_{12}$ . We have checked that such a Mott-Jones term is not relevant either in  $\text{LaFe}_4\text{Sb}_{12}$  to fit the resistivity data at high temperature.

The fit of the resistivity curve by equation (5) is quite good, but it involves three fitting parameters, so that the agreement cannot be considered as a definite proof of validity of the analysis. Moreover, equation (5) is just the addition of independent terms, which corresponds to the Matthiessen rule. However, in filled skutterudites in general, and in  $\text{LaFe}_4\text{Sb}_{12}$  in particular, the total resistivity is a substantial fraction of the maximum value obtained when the mean free path of the free carriers is of the order of the lattice parameter (roughly the Ioffe-Regel limit). In this case the Matthiessen rule is broken [35], and its violation will also be responsible for saturation effects in the  $\rho(T)$  curve. Even without invoking the breakdown of the Matthiessen rule, should the resistivity show tendency toward saturation as one approaches the Ioffe-Regel limit [36]. It explains for example, why such a lanthanide superconductor as  $\text{LaAl}_2$  also has a large and S-shaped resistivity curve similar to that of  $\text{LaFe}_4\text{Sb}_{12}$ , despite the lack of any transition element [37]. In  $\text{LaAl}_2$ , the electron-phonon interaction alone has then to be invoked to explain the large and S-shaped resistivity. The situation in A15 transition metals is a more ambiguous example, as it is not clear whether such similar resistivity curves are attributable to the scattering of the electrons by spin fluctuations, or by the electron-phonon interaction as it has been suggested in the past [35]. Therefore, the attribution of the large and S-shaped resistivity curve in  $\text{LaFe}_4\text{Sb}_{12}$

is still an open question. For all these reasons, our analysis of  $\rho(T)$  at  $T > T_{\text{inf}}$  according to equation (5) remains questionable, and we can only assert that the temperature dependence of the resistivity at these high temperatures is compatible with the behavior expected within spin fluctuation theory. Let us point out, however, that in the case the saturation effects are attributable to the approach of the Ioffe-Regel limit, the resistivity can be fit by a parallel transistor formula  $\rho(T) = [1/\rho_\infty + 1/(\rho'T)]^{-1}$  with  $\rho'$  a constant [38]. We have checked that this law, which has been found of remarkable accuracy in such a case [39], does not fit our data for  $\text{LaFe}_4\text{Sb}_{12}$ , with fitting parameters  $\rho_\infty$  and  $\rho'$  kept in a physical range of values. This result then pleads in favor of the attribution of the S-shaped resistivity curve  $\text{LaFe}_4\text{Sb}_{12}$  to spin fluctuation effects.

The analysis at low temperature  $T < T_{\text{inf}}$  does not suffer such difficulties, since the electron-phonon scattering becomes much smaller, and the Matthiessen rule applies. We can then write safely that the total resistivity at low temperature is the sum of  $\rho(0)$  originating from the scattering by impurities, plus the part  $\rho_{\text{sf}}$  due to spin fluctuations. The same spin fluctuation theory which we used to analyze the magnetic susceptibility [25] predicts that  $\rho_{\text{sf}} \propto T^\alpha$ , with  $\alpha = 5/3$  for ferromagnetic spin fluctuations, and  $\alpha = 3/2$  for antiferromagnetic fluctuations at  $d = 3$ , against the classical exponent  $\alpha = 2$ . The temperature dependence of  $\rho_{\text{sf}} = \rho(T) - \rho(0)$  in a log-log scale is reported in Figure 5. The power-law is well satisfied, and the parameter  $\alpha$  deduced from a least square fit is  $\alpha = 1.7$  close to  $5/3$ , which is another proof that the NFL behavior is governed by ferromagnetic spin fluctuations. Data in Figure 5 have been also reported at  $T > T_{\text{inf}}$ , although the power-law is meaningless at these high temperatures, to illustrate the deviation of  $\rho(T)$  from this power law above  $T_{\text{inf}}$ . It is another evidence that above this temperature, the resistivity is dominated by the phonons (see Fig. 4 and previous paragraph), and not by the spin fluctuations. It is also consistent with the fact that  $T_{\text{inf}}$  is a measure of the spin fluctuation temperature [31].

## 4.2 Magnetotransport

The magnetoresistivity at low temperature is illustrated in Figure 6.  $\rho(H) - \rho(H = 0)$  is positive, and saturates at  $H \simeq 3$  Teslas at  $T = 4.2$  K. The measurements up to 22 Teslas at 4.2 K (not reported in Fig. 6) show that  $\rho(H)$  does not depend on  $H$  between 6 and 22 Teslas. At  $T > 20$  K, however, an additional contribution takes place. This case is illustrated in Figure 6 at  $T = 30$  K. On another hand, the contribution from spin fluctuations in a NFL regime is expected to be negative in the case of ferromagnetic fluctuations [40]. We can then understand the magnetoresistivity, assuming the existence of three contributions: (a) a positive contribution which saturates at  $H \simeq 3$  Teslas; (b) a positive contribution, which does not saturate up to 6 Teslas; (c) a negative contribution associated to the spin fluctuations according to the theoretical predictions [40].

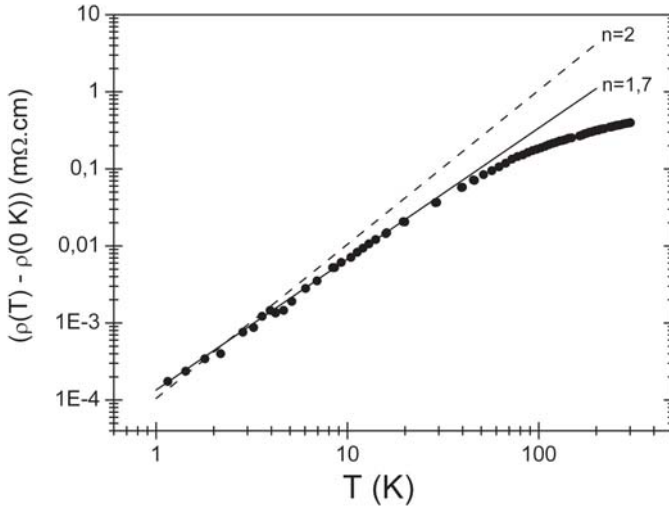


**Fig. 5.** Temperature dependence of  $\rho(T) - \rho(T \rightarrow 0)$  in log-log scale at low temperature for the batch 1 sample. The dots are experimental data. The solid and broken lines correspond to different power laws  $T^n$ .  $n = 2$  (broken line): Fermi liquid behavior,  $n = 1.7$  which fits the data (full line): non-Fermi liquid behavior of  $\text{LaFe}_4\text{Sb}_{12}$ .

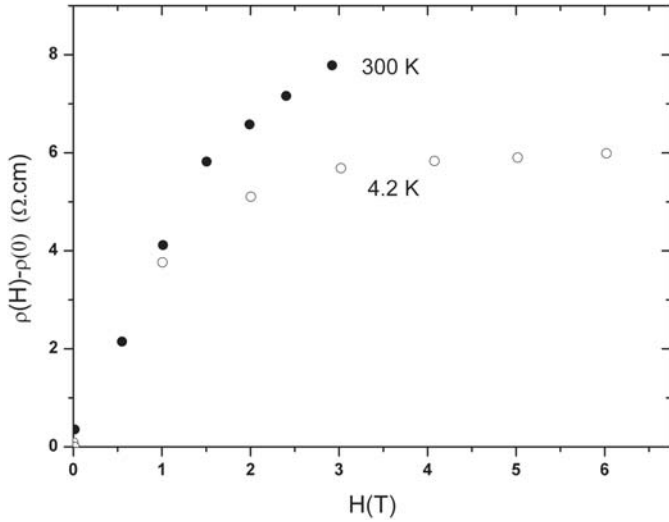


**Fig. 6.** Magnetoresistance  $\rho(H) - \rho(H = 0)$  of the batch 1 sample as a function of the magnetic field  $H$  at different temperatures.

Let us now discuss the mechanisms at the origin of this behavior. The contributions (a) and (b) are features met in metals, whether they are transition metals or not [41,42]. Both are contributions from impurities and defects. The saturating component is related to microscopic inhomogeneities or local defects, the non-saturating component originates from spatial inhomogeneities at a macroscopic scale. This analysis is corroborated by measurements of the Hall resistivity  $\rho_H$  reported in Figure 7. At 4.2 K,  $\rho_H$  is linear in  $H$  only at a field  $H > 2$  Teslas, so that both  $\rho_H$  and  $\rho(H)$  show a crossover behavior at about the same field 2–3 Teslas. Such a correlation between saturation in the magnetoresistivity and change of slope in

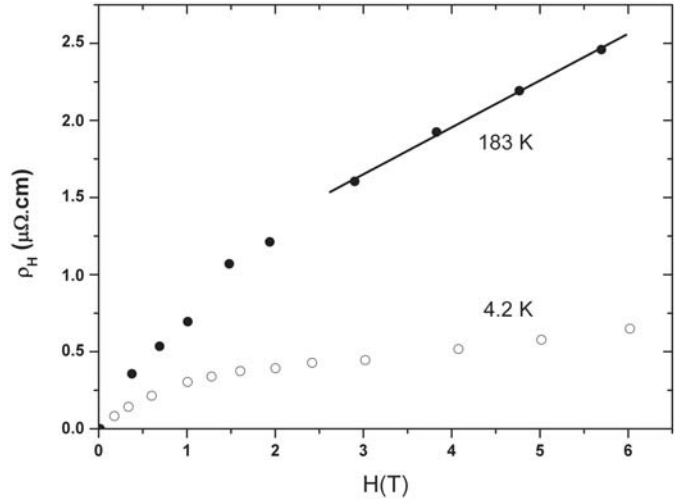


**Fig. 7.** Hall resistivity  $\rho_H$  of the batch 1 sample as a function of the magnetic field  $H$  at different temperatures. The solid line is the fit of  $\rho_H(H)$  in the linear regime at high temperature, and corresponds to a hole concentration per formula unit  $p = 0.8$ .

the field-dependence of the Hall resistivity has been already observed in K-metals [41], as a result of impurities and defects. We are led to the same conclusion for the case of  $\text{LaFe}_4\text{Sb}_{12}$ . Note these two processes are mainly independent of temperature, so that the increase of the magnetoresistivity above 20 K can be attributed to a decrease (in absolute value) of the contribution (c), as  $T$  increases. The fact that the spin fluctuations are not negligible may also explain the decrease of the slope of  $\rho_H(T)$  as  $T$  decreases, which can be observed in Figure 7. This effect may be attributable to a non negligible anomalous Hall effect expected in this nearly ferromagnetic metal. As a consequence, the free carrier concentration is best deduced from the slope of  $\rho_H(H)$  at high field measured at high temperature. It is found equal to  $p = 0.8$  hole per formula from the  $\rho_H(H)$  curve at  $T = 185$  K displayed in Figure 7. This compares well the occupation rate 0.9 of the rare earth site in our samples, as deduced from chemical and microprobe analysis. Such a deficiency with respect to the theoretical value  $p = 1$  is observed in all the filled skutterudites, since the filling of the rare earth ion sites is incomplete [43].

For completeness, let us mention that we have also explored the hypothesis of a field dependence of  $\rho_H(H)$  and  $\rho(H)$  due to the existence of two carriers, say heavy and light free carriers, which would coexist in the vicinity of a peak of density of states at the Fermi level. We have checked however, that the dependence of  $1/(R_H - R_0)$  on  $H^{-2}$  and  $1/(R_H - R_\infty)$  on  $H^2$  are not straight lines, as they should if the Chambers formulas would apply (see Ref. [44] and references therein, for instance). This rules out the hypothesis that the magnetic dependence of the transport properties we have observed are attributable to a two-band effect. In addition, we expect the hybridization between  $s$  and  $p$  states to be too strong in these materials to generate such effects.

To conclude this section, we have found indirect evidence of spin fluctuation effects on both the magnetoresistivity and the Hall effect. The contribution from spin fluctuations to the magnetotransport, however, could not be determined quantitatively, as it is clearly not the dominant mechanism which rules the magnetotransport process.

## 5 Thermal properties

### 5.1 Heat capacity

The thermal variation of the heat capacity  $C_p$  of LaFe<sub>4</sub>Sb<sub>12</sub> below 10 K is reported in Figure 8 at  $H = 0$  and under a high magnetic field  $H = 9$  Teslas. We expect  $C_p$  to satisfy the Grüneisen-Bloch relation:

$$C_p = (\gamma_e + \gamma_s)T + \beta T^3. \quad (6)$$

As usual the first term  $\gamma_e T$  is the free carrier contribution and  $\beta T^3$  is the phonon contribution. The contribution of the spin fluctuations to the heat capacity includes a first-order (leading term)  $\gamma_s T$ , while the second-order term, in non-Fermi liquids, is of the form  $-cT \ln T$  for ferromagnetic spin fluctuations ( $-cT^{3/2}$  for antiferromagnetic spin fluctuations) at  $d = 3$  [25]. The temperature dependence of this second-order term is the result of the self-consistent renormalization theory, and must be understood at the asymptotic limit  $T \rightarrow 0$ . In practice, this term will be important enough to dominate the other contributions only at very low temperature (typically 0.1 K) so that we can omit it in first approximation and consider only equation (6). That is why the experimental results are reported in Figure 7 as  $C_p/T$  versus  $T^2$ . The linear behavior in this representation shows that equation (6) is well satisfied in the range  $0.8 < T < 6$  K. From the interpolation of this linear variation down to  $T = 0$ , we find:

$$\gamma = \gamma_e + \gamma_s = 195 \text{ mJ/mole K}^2, \quad (7)$$

in agreement with previous measurements [4].

A quantitative comparison with CeFe<sub>4</sub>Sb<sub>12</sub> is made difficult by the anomalous behavior of  $C_p$  at low temperature in this compound. In particular, two different estimations of  $\gamma$  can be made, depending on the temperature range considered for the analysis of  $C_p(T)$ :  $\gamma = 63.8$  mJ/moleK<sup>2</sup> in the range  $6.3 < T < 10$  K [6], against  $\gamma = 180$  mJ/moleK<sup>2</sup> estimated by the same authors [6] from the data at  $T = 2$  K. If we retain the lower value 63.8, the value of  $\gamma$  is twice as big in LaFe<sub>4</sub>Sb<sub>12</sub> as in CeFe<sub>4</sub>Sb<sub>12</sub>. This is at contrast with the common rule in rare earth compounds, according to which the substitution Ce  $\rightarrow$  La decreases  $\gamma$ . If we retain the larger value 180, we find that both compounds have roughly the same  $\gamma$ .

The total quenching of the spin fluctuation contribution by the magnetic field results in a shift of the  $C_p/T$  curve by an amount  $\gamma_s$ . If the field  $H = 9$  Teslas were sufficient to totally quench the spin fluctuations,

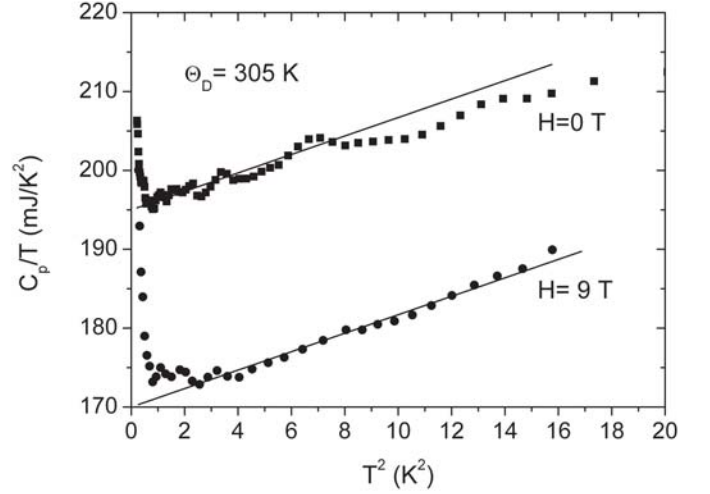


**Fig. 8.** Heat capacity  $C_P$  as a function of  $T^2$  where  $T$  is the temperature without any applied magnetic field ( $H = 0$ ) and under a magnetic field  $H = 9$  Teslas applied to the batch 1 sample. The solid line corresponds to the Grüneisen-Bloch law in equation (6) with the Debye temperature  $\theta_D = 305$  K determined by ultrasonic measurements [17].

the 26 mJ/moleK<sup>2</sup> shift between the two curves in Figure 8 would be equal to  $\gamma_s$ . As the quenching is not total, this shift is an underestimation of this parameter, so that

$$\gamma_e < 169 \text{ mJ/mole K}^2, \quad \gamma_s > 26 \text{ mJ/mole K}^2. \quad (8)$$

An anomalously large value of  $\gamma_e$  can be explained on the basis of band structure calculations [45] which predict an important free carrier concentration  $n(E_f)$  at the Fermi level in other skutterudites filled with La, which have  $\gamma_e$  in the range 20–60 mJ/moleK<sup>2</sup> [33]. The prediction for LaFe<sub>4</sub>Sb<sub>12</sub> is  $\gamma_e = 62$  mJ/moleK<sup>2</sup> against  $\gamma_e = 32$  mJ/moleK<sup>2</sup> in LaFe<sub>4</sub>P<sub>12</sub> [45]. For this last material, the experimental value is  $\gamma_e = 57$  mJ/moleK<sup>2</sup>. Since the calculated values of  $\gamma_e$  in [45] are found to reproduce the relative variations of this parameter among the series of skutterudites filled with La, we expect that the theoretical and experimental values change in the same proportions between LaFe<sub>4</sub>Sb<sub>12</sub> and LaFe<sub>4</sub>P<sub>12</sub>. In LaFe<sub>4</sub>Sb<sub>12</sub>, we then estimate  $\gamma_e = (57/32) \times 62 = 110$  mJ/moleK<sup>2</sup>, and taking equation (7) into account:

$$\gamma_e = 110 \text{ mJ/mole K}^2, \quad \gamma_s = 85 \text{ mJ/mole K}^2. \quad (9)$$

This is compatible with equation (8) and the best guess we can have for these two parameters.  $\gamma_s$  is then of the same order of magnitude as  $\gamma_e$ , and thus anomalously large too. According to the predictions of spin fluctuation theory,  $\gamma_s$  remains small near an antiferromagnetic instability [46], but large as one approaches a ferromagnetic instability [47]. The large value of  $\gamma_s$  is then an additional proof that LaFe<sub>4</sub>Sb<sub>12</sub> is near a ferromagnetic instability.

Finally we note that, taking into account the effective magnetic moment deduced from the effective Curie constant, we can determine the Wilson ratio  $R_w = \pi^2 k_B^2 \chi(T \rightarrow 0) / (\mu_{\text{eff}}^2 \gamma)$ . We find  $R_w = 4.6$ . Such a

large value of  $R_w$  is expected for systems dominated by ferromagnetic spin fluctuations [48]. The largest Wilson ratio in paramagnets has indeed been observed in the case of ferromagnetic spin fluctuations, with  $R_w \geq 10$  in  $\text{Sr}_3\text{Ru}_2\text{O}_7$  [49]. However, this material is quasi-two-dimensional, while  $\text{LaFe}_4\text{Sb}_{12}$  is three dimensional. In addition, Wilson ratios comparable to that of  $\text{LaFe}_4\text{Sb}_{12}$  can be met in other systems where spin fluctuations are not necessarily ferromagnetic. For instance, in the Brinkman-Rice picture for the Hubbard model on the metallic side near a metal-insulator transition,  $R_w = 4$  [50]. The common feature of all these systems is that large values of  $R_w$  result from spin fluctuations which are enhanced with respect to the Fermi liquid. We then conclude that the value of  $R_w = 4.6$  we have determined for  $\text{LaFe}_4\text{Sb}_{12}$  is another evidence that the physical properties of this material are dominated by spin fluctuations. This value of  $R_w$  is not a proof that these spin fluctuations are ferromagnetic, but it is actually compatible with such a nature of the spin fluctuations.

The slope  $\beta$  of the  $C_p/T$  as a function of  $T^2$  in Figure 8 is roughly independent of  $H$  as expected, as it is related to the phonon contribution. Its value  $1.0 \text{ mJ}/(\text{mole K}^4)$  is in agreement with a prior result [51]. From  $\beta$ , we can deduce the Debye temperature  $\theta_D$ , using the formula:  $\theta_D = [(12\pi^4 NR)/(5\beta)]^{1/3}$ , where  $R$  is the universal gas constant, and  $N$  is the number of atoms per formula unit.  $N$  is in the range 16.8–16.9, lower than 17, due to the fact that the filling ratio of the rare earth site is slightly smaller than unity. We find  $\theta_D = 305 \text{ K}$ . This value is smaller than the value  $348 \text{ K}$  reported in reference [4], but in quantitative agreement with the value deduced from ultrasonic experiments [17], and closer to the value  $\theta_D = 250 \text{ K}$  reported for  $\text{CeFe}_4\text{Sb}_{12}$ . Indeed, the phonon spectra are comparable in both materials, and so must be the Debye temperatures.

A deviation with respect to equation (6) can be observed at  $T > 10 \text{ K}$  at  $H = 0$  in Figure 8, which comes from the fact that the deviation of the Grüneisen-Bloch law with respect to the first order term  $\beta T^3$  is negligible only at  $T < \theta_D/50$  [52].

On another hand, the upward curvature of  $C_p/T$  upon cooling at low temperature in Figure 8 is of a different nature. To characterize this effect, we have reported in Figure 9 the difference  $C_N$  between the experimental specific heat and the the Grüneisen-Bloch law as given by equations (6, 7) as a function of  $T$  in a log-log plot. This plot gives evidence of a  $T^{-2}$  power law for  $C_N$ :

$$C_N = A_N T^{-2}, \quad (10)$$

which behavior is characteristics of a Schottky anomaly [53]. The least square fit materialized by the solid lines in Figure 9 gives  $A_N = 1.2 \text{ mJ K}/\text{mole}$  at  $H = 0$ , and raises to  $4.2 \text{ mJ K}/\text{mole}$  at  $H = 9 \text{ Teslas}$ . We cannot rule out the possibility that it is due to some impurity. However, the measurements of the thermal properties have been made on the sample (batch 1) defined earlier in this work as the best sample available, according to both the magnetic properties and the metallographic characterization. We then consider that the

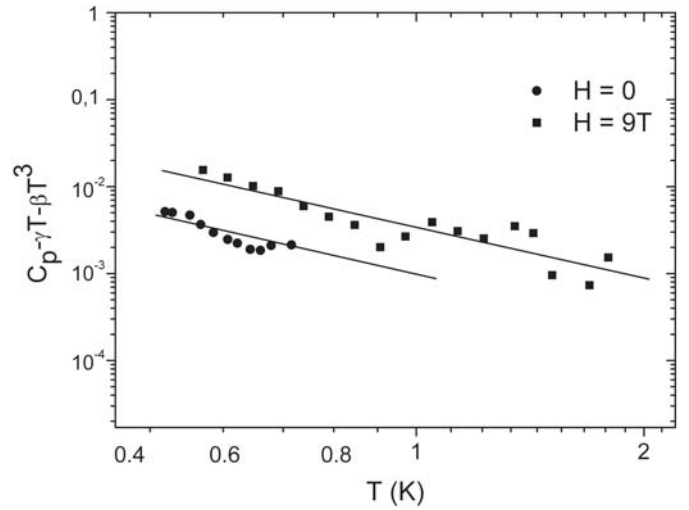


**Fig. 9.** Nuclear heat capacity  $C_N$  as defined by the difference between the experimental heat capacity and the Grüneisen-Bloch contribution (see Eq. (6)) for the batch 1 sample. The  $T^{-2}$  behavior is materialized by the solid lines.

effect is more likely an intrinsic property, and originates from a nuclear Schottky anomaly due to the hyperfine-split ground states of the nuclei. Since the maximum of this Schottky contribution is at a temperature smaller than the temperatures available in the experiments, it is sufficient to keep the lowest-order term in the general expansion in inverse power of  $T$  to obtain the nuclear contribution  $C_N$  of the specific heat under the form [53]:

$$A_N/R = \frac{I_e(I_e + 1)}{3I_e^2} \sum_{i,e} \nu_e^i [g(I_e)\mu_N H_{\text{eff}}(e)/k_B]^2 \quad (11)$$

plus a quadrupole contribution which is negligible here. In this equation,  $\nu_e^i$  is the abundance of the isotope  $i$ ,  $I_e$  is the nuclear spin,  $\mu_N$  the nuclear magneton,  $g(I_e)$  the gyromagnetic factor and  $H_{\text{eff}}(e)$  the effective hyperfine magnetic field at the nucleus of the element  $e = \text{La, Fe, Sb}$ . In most elements, the contribution of the nucleus is typically the order of  $10^{-5} \text{ J K}/\text{mole}$ . The case of Sb, however, is anomalous. In the uranium mononictides for instance, the coefficient  $A_N$  has been measured and found equal to few  $10^{-5} \text{ J K}/\text{mole}$  just like in uranium monochalcogenides, except in USb, where  $A_N = 1.44 \text{ mJ K}/\text{mole}$  [54]. The Sb contribution of Sb to  $A_N$  (contribution of  $e = \text{Sb}$  in Eq. (11)) has been calculated in [54] from the value of  $H_{\text{eff}}$  given in [55]. The result is  $1.3 \text{ mJ K}/\text{mole}$ , which is in very good agreement with the experimental value of  $A_N$  we have determined in  $\text{LaFe}_4\text{Sb}_{12}$ . This also corroborates that the Schottky anomaly is attributable to the excitations between hyperfine-split nuclear energy levels, the largest contribution coming from the *Sb* nucleus.

The spin fluctuation theory of non-Fermi liquid behavior predicts a  $-T \ln T$  behavior of the specific heat at low temperature [56], in the case of ferromagnetic spin fluctuations. One consequence of the nuclear contribution evidenced in this work is that it makes impossible the detection of such a  $-T \ln T$  contribution, as it is negligible with



respect to a sharp increase of  $C_p$  in  $T^{-2}$ . Even if a  $-T \ln T$  term exists, it might be detected only at lower temperatures such that  $k_B T$  is smaller than the Zeeman energy splitting of the nuclear ground state, i.e below the maximum of the nuclear Schottky anomaly. In practice, this condition requires the investigation of the specific heat at temperatures below 0.1 K, which were not available with our experimental set-up.

## 5.2 The Grüneisen parameter

The study of the Grüneisen parameter  $\Gamma$  is of great interest in transition metals, since it is more sensitive to spin fluctuation effects than the specific heat itself. In materials where spin fluctuations are negligible, including transition metals [57] and minerals as well [58],  $\Gamma$  is usually between 1–2 at low temperature. On another hand, when spin fluctuations are important, they can raise significantly  $\Gamma$  at low temperatures. Close to a quantum critical point,  $\Gamma$  is even expected to diverge [59]. Indeed a power law divergence  $\Gamma \propto T^{-x}$  has been observed at least in two compounds CeNi<sub>2</sub>Ge<sub>2</sub> and YbRh<sub>2</sub>(Si<sub>0.95</sub>Ge<sub>0.05</sub>)<sub>2</sub>, with  $x = 1$  and  $x = 0.7$ , respectively [60].

As already stated in Section 2, the heat capacity  $C_v$  entering the definition of  $\Gamma = 3\alpha_T B_T V / C_v$  is at constant volume, while we have measured the heat capacity at constant pressure  $C_p$ . The difference  $C_p - C_v = 9\alpha_T^2 B_T V T$  is however negligible in the range of temperatures investigated, and we then write  $\Gamma = 3\alpha_T B_T V / C_p$ . We assume that the bulk modulus  $B_T$  is temperature independent, and equal to the value  $8.4 \times 10^{10}$  N/m<sup>2</sup> of this parameter in LaFe<sub>3</sub>CoSb<sub>12</sub>. Since this compound differs from LaFe<sub>4</sub>Sb<sub>12</sub> only by the substitution of one Fe atom out of four by one Co, this is a reasonable assumption, inasmuch as  $B_T$  is about the same in the unfilled skutterudite CoSb<sub>3</sub> [61]. From the measurements of the heat capacity reported in the previous section, measurements of the thermal expansion coefficient  $\alpha_T$  as a function of  $T$ , reported in Figure 10 allows for the determination of  $\Gamma$ . The results are reported in Figure 11. At  $T > 60$  K,  $\Gamma$  does not depend on temperature, and is equal to 1.5, which gives evidence that spin fluctuations are negligible at such temperatures. As  $T$  decreases below 60 K, however,  $\Gamma(T)$  increases upon cooling.

One hypothesis is that this effect is due to the additional contribution of spin fluctuation effects which become important below the spin fluctuation temperature  $T_{sf}$ . The log-log plot in Figure 9 is in agreement with the  $T^{-x}$  diverging behavior expected for spin fluctuations near the critical point, with  $x \simeq 2/3$ .

On one hand, there are theoretical arguments to explain this value of  $x$ . The problem of an electron gas interacting via exchanging transverse gauge bosons has been addressed by Gan and Wong [62]. These authors have determined that the long wavelength behavior of the gauge field is in the Gaussian universality class with a dynamic exponent  $z = 3$  in dimension  $d \geq 2$ . This result should apply in particular, if the role of the gauge field is played by the soft (paramagnon) mode of a nearly ferromagnetic

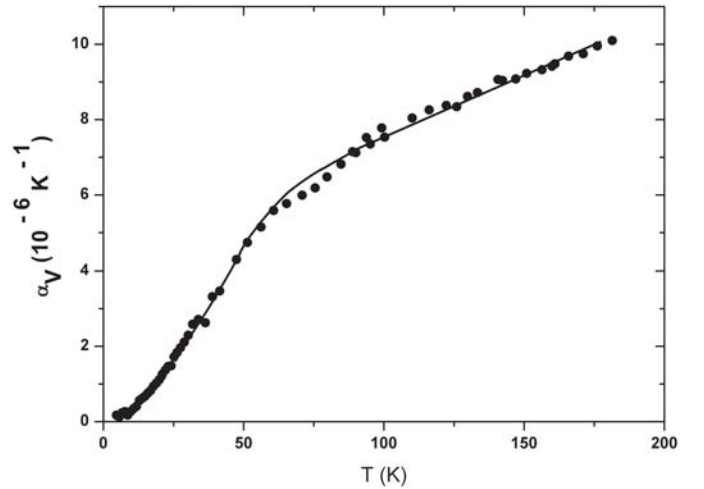


**Fig. 10.** Temperature dependence of the dilatation coefficient of the batch 1 sample. The solid line is a guide for the eyes.

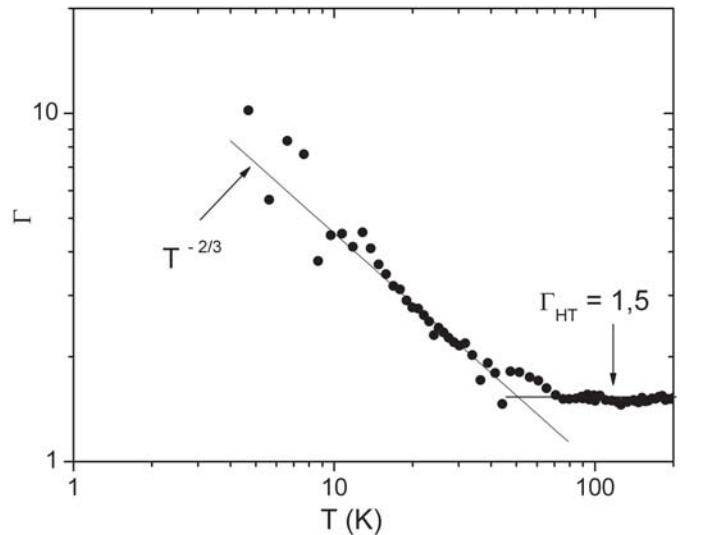


**Fig. 11.** Temperature dependence of the Grüneisen parameter  $\Gamma(T)$  of the batch 1 sample, in log-log scale. The solid line corresponds to a power law  $T^n$  with  $n = -2/3$  ( $T < 50$  K), and a constant ( $T > 50$  K).

material. In the Gaussian universality class, the critical exponent for the correlation length is  $\nu = 1/2$  [63]. When scaling applies,  $x = 1/(z\nu)$  [59], which, combined with  $\nu = 1/2, z = 3$ , leads to  $x = 2/3$ . We find the same result if we note that, according to the theory, the spin fluctuations will contribute a term in  $T^{1/3}$  which will dominate the temperature dependence of  $\alpha_T$  at low temperature [59]. Since we are in the temperature range where the heat capacity is dominated by  $\gamma T$ , after Section 5.1, we then expect  $\Gamma \propto \alpha_T / C_p \propto T^{-2/3}$ , in agreement with the result in Figure 5.

On another hand, it should be reminded here that this analysis should apply only to the critical part  $\Gamma_c$  of  $\Gamma$ . A better approach would then be to write  $\Gamma(T) = \Gamma_0 + \Gamma_{cr}$ , with  $\Gamma_0$  a constant.  $\Gamma_0$  is expected to be smaller than the high temperature value of  $\Gamma(T)$ , but may actually be non

negligible at  $T > 4$  K. Measurements below 4 K, however, are prohibited, mainly because both  $\alpha_T$  and  $C_v$  vanish at  $T = 0$ , so that the error bars in the determination of the Grüneisen parameter ( $\propto \alpha_T/C_v$  increases upon cooling (and will eventually diverge at  $T = 0$ ). This is the reason why the dispersion of the data points becomes large below 10 K, and also the reason why this parameter is always investigated at higher temperatures in the literature. We have checked that the subtraction of a constant term to  $\Gamma$  in the plot of Figure 9 does not alter the fit by a power law, but only increases the fitting parameter  $x$ . We then consider the value  $x = 2/3$  as the lower limit for this parameter in  $\text{LaFe}_4\text{Sb}_{12}$ .

For completeness, let us discuss another hypothesis. The low-frequency motion of the rare earth ions inside the cages of the skutterudite may be responsible for an unusual low-temperature anharmonicity resulting in an unusual increase of  $\Gamma$  upon cooling at low temperature. This effect has been observed in clathrates [64, 65] and clathrate hydrates [66], another family of materials in which the host forms cages inside which the guest atoms “rattle”. However, no theoretical model supports that the temperature dependence of  $\gamma$  should be a power law in this case. On an experimental point of view, to our knowledge, no such a power law has ever been reported, neither in the clathrate family nor in other materials with low-frequency librational modes [67]. Furthermore, the Sommerfeld coefficient  $\gamma$  of the specific heat is small in clathrate compounds [68], which means that the phonons dominates the thermal properties of these materials at low temperature. This is not the case in  $\text{LaFe}_4\text{Sb}_{12}$  where the large value of  $\gamma$  means low temperature thermal properties dominated by the free carriers and their spin fluctuations. Finally, inelastic neutron scattering [69] and first principle calculations as well [70] show that the anharmonicity associated to the rattling effect is very weak in  $\text{LaFe}_4\text{Sb}_{12}$ . On the basis of these concordant arguments, we conclude that the  $T^{-x}$  power law observed for the Grüneisen parameter of this compound with  $x \geq 2/3$  is the evidence of spin fluctuations. In addition the onset of this power law at  $T_{sf} \simeq 60$  K gives another independent determination of the spin fluctuation temperature.

## 6 Discussion

The study of the resistivity, magnetic susceptibility, heat capacity and Grüneisen parameter measurements gives evidence that  $\text{LaFe}_4\text{Sb}_{12}$  belongs to the family of strongly correlated fermion systems, due to the  $d$ -electrons of the iron. The spin fluctuations dominate the physical properties at low temperature, and the spin fluctuation temperature can be estimated from the effective Curie temperature  $\theta \simeq 50$  K, the temperature  $T_{\text{inf}} \simeq 65$  K of the inflection point of the resistivity curve, and the crossover behavior of the Grüneisen parameter at  $T \simeq 60$  K.

This result provides us with a new understanding of the physical properties of this material reported in the literature, such as the temperature dependence of the Seebeck coefficient  $S(T)$  [4].  $S(T)$  is positive at high temperature, as it should since the metallic character of

$\text{LaFe}_4\text{Sb}_{12}$  is due to holes. But  $S(T)$  decreases as  $T$  decreases, changes sign at  $T \simeq 90$  K, and goes through a (negative) minimum at  $T_{\text{min}} \simeq 35$  K. Such a negative minimum is also observed in other nearly magnetic alloys such as Pd-Ni and Rh-Fe where it has been attributed to spin fluctuations effects [71] with  $T_{\text{sf}}$  in the range  $1-2 T_{\text{min}}$  [71, 72]. In addition, while there is an experimental evidence that  $\text{LaFe}_4\text{Sb}_{12}$  is not magnetic, recent spin-polarized band calculations support a magnetic solution [73]. This is due to the fact that this compound is actually close to a magnetic instability at  $T = 0$ , at the origin of the NFL behavior.

Power laws observed for the temperature dependence of the resistivity, magnetic susceptibility, Grüneisen parameter show that  $\text{LaFe}_4\text{Sb}_{12}$  is close to a magnetic instability. Moreover, the values of the exponents suggest that the dominant spin fluctuations are of the ferromagnetic type. This result is also supported by the heat capacity measurements showing an anomalously large  $\gamma$  parameter, and magneto-transport properties such as non linearity in the magnetization curves. We then conclude that an overall understanding of the magnetic susceptibility together with the electron and heat transport properties of  $\text{LaFe}_4\text{Sb}_{12}$  has been achieved, and that this material is close to a ferromagnetic instability, with a spin fluctuation temperature  $T_{sf} = 50 \pm 15$  K.

## References

1. C. Uher, *Semicond. and Semimet.* **69**, 139 (2001), and refs. therein
2. E. Bauer, St. Berger, A. Galatanu, Ch. Paul, M. Delle Mea, H. Michor, G. Hilscher, A. Grytsiv, P. Rogl, D. Kaczorowski, L. Keller, T. Hermannsdörfer, P. Fischer, *Physica B* **312–313**, 840 (2002)
3. M.E. Danebrock, C.B.H. Evers, W. Jeitschko, *J. Phys. Chem. Solids* **57**, 381 (1996)
4. E. Bauer, St. Berger, A. Galatanu, M. Galli, H. Michor, G. Hilscher, Ch. Paul, *Phys. Rev. B* **63**, 224414 (2001)
5. M.S. Torikachvili, J.W. Chen, Y. Dalichaouch, R.P. Guertin, M.W. McElfresh, C. Rossel, M.B. Maple, *Phys. Rev. B* **36**, 8660 (1987)
6. D.A. Gajewski, N.R. Dilley, E.D. Bauer, E.J. Freeman, R. Chau, M.B. Maple, D. Mandrus, B.C. Sales, A.H. Lacerda, *J. Phys. C: Condens. Mater.* **10**, 6973 (1998)
7. R. Viennois, D. Ravot, J.C. Tedenac, S. Charar, A. Mauger, *Mater. Sci. Eng. B*, in press
8. . Leithe-Jasper, D. Kaczorowski, P. Rogl, J. Bogner, M. Reissner, W. Steiner, G. Wiesinger, C. Godart, *Slid Stat. Commun.* **109**, 365 (1999)
9. N.R. Dilley, E.J. Freeman, E.D. Bauer, M. Maple, *Phys. Rev. B* **58**, 6287 (1998)
10. T.D. Matsuda, H. Okada, H. Sugawara, Y. Aoki, H. Sato, A.V. Andreev, Y. Shiokawa, V. Sechovsky, T. Honma, E. Yamamoto, Y. Onuki, *Physica B* **281–282**, 220 (2000)
11. H. Sugawara, Y. Abe, Y. Aoki, H. Sato, M. Hedo, R. Settai, Y. Onuki, H. Harima, *J. Phys. Soc. Jpn.* **69**, 2938 (2000)
12. E. Bauer, St. Berger, M. Delle Mea, G. Hilscher, H. Michor, Ch. Paul, A. Grytsiv, P. Rogl, E.W. Scheid, C. Godart, M. Abd Elmeguid, *Acta Phys. Pol. B* **34**, 595 (2003) and refs. therein

13. L. Chapon, D. Ravot, J.C. Tedenac, J. Alloys Compds **299**, 68 (2000)
14. D. Ravot, U. Lafont, L. Chapon, J.C. Tedenac, A. Mauger, J. Alloys Compds **323-324**, 389 (2001)
15. R. Viennois, F. Terki, A. Errebah, S. Charar, M. Averous, D. Ravot, J.C. Tedenac, P. Haen, C. Sekine, Acta Physica Polonica B **34**, 1221 (2003)
16. G.J. Long, D. Hautot, F. Grandjean, D.T. Morelli, G.P. Meisner, Phys. Rev. B **60**, 7410 (1999)
17. B.C. Sales, B.C. Chakoumakos, D. Mandrus, Proc. Mat. Res. Soc. Symp. **626**, Z7.1.1 (2000)
18. H. Sato, Y. Abe, H. Okada, T. Matsuda, H. Sugawara, Y. Aoki, Physica B **281**, 306 (2000)
19. N. Takeda, M. Ishikawa, Physica B **259-261**, 92 (1999); Physica B **281-282**, 388 (2000); J. Phys. C: Condens. Matter **13**, 5971 (2001)
20. L. Chapon, D. Ravot, J.C. Tedenac, J. Alloys Compds **282**, 58 (1999)
21. R. Viennois, Ph. D. thesis, Universite Montpellier II (2002)
22. C. Herring, in *Magnetism*, edited by G. Rado, H. Suhl (Academic, New York, 1965), Vol. 2A
23. T. Moriya, *Spin Fluctuations in Itinerant Electron Magnetism* (Springer, Berlin, 1985)
24. G.R. Stewart, Rev. Mod. Phys. **73**, 797 (2001)
25. T. Moriya, T. Takimoto, J. Phys. Soc. Jpn. **64**, 960 (1995)
26. P. Coleman, Physica B **259-261**, 353 (1999)
27. Q. Si, J.L. Smith, K. Ingersent, Int. J. Mod. Phys. B **13**, 2331 (1999)
28. A. Mauger, J. Ferré, P. Beauvillain, Phys. Rev. B **40**, 862D864 (1989), and references therein
29. F. Rivadulla, M. Banobre-Lopez, M.A. Lopez-Quintela, J. Rivas, cond-mat/0403687
30. G. Gumbs, A. Griffin, Phys. Rev. B **13**, 5054 (1976)
31. J.M. Lawrence, P.S. Riseborough, R.D. Parks, Rep. Prog. Phys **44**, 1 (1981)
32. N. Rivier, V. Zlatic, J. Phys. F: Metal Phys. **2**, L99 (1972)
33. I. Shirovani, K. Ohno, C. Sekine, T. Yagi, T. Kawakami, T. Nakanishi, H. Takahashi, J. Tang, A. Matsuchita, T. Matsumoto Physica B **281-282**, 1021 (2000), and references therein
34. D.W. Woodard, G.D. Gody, Phys. Rev. A **136**, 166 (1966)
35. Z. Fisk, G. Webb, Phys. Rev. Lett. **36**, 1084 (1976)
36. M. Calandra, O. Gunnarsson, Phys. Rev. B **66**, 205105 (2002)
37. H.J. Van Daal, K.H.J. Bushow, Phys. Stat. Solidi A **3**, 853 (1970)
38. F.P. Mena, D. van der Marel, A. Damascelli, M. FLth, A.A. Menovsky, J. A. Mydosh, Phys. Rev. Lett. **38**, 782 (1977)
39. F.P. Mena, D. Van der Marel, A. Damscelli, M. Fäth, A.A. Menowsky, J.A. Mydosh, Phys. Rev. B **67**, 241101 (2003)
40. T. Moriya, J. Magn. Magn. Mat. **14**, 1 (1979)
41. J. Babiskin, P.G. Siebermann, Phys. Rev. Lett. **27**, 1361 (1971); P.G. Siebermann, J. Babiskin, Phys. Rev. Lett. **30**, 380 (1973)
42. A.B. Pippard, *Magnetoresistance in Metals*, (Cambridge University Press, New York, 1989)
43. J.W. Kaiser, W. Jeitschko, J. Alloys and Comp. **66**, 291 (1999)
44. E. Arushanov, Ch. Kloc, H. Hohl, E. Bucher, J. Appl. Phys. **75**, 5106 (1994)
45. H. Harima, J. Magn. Magn. Mater. **177-181**, 321 (1998)
46. T. Moriya, Phys. Rev. Lett. **24**, 1433 (1970)
47. S. Doniach, S. Engelsberg, Phys. Rev. Lett. **17**, 750 (1966)
48. M.A. Continentino, Phys. Rev. B **55**, 5589 (1997)
49. S.-H. Ikeda, Y. Maeno, S. Nakatsuji, M. Kosaka, Y. Uwatoko, Phys. Rev. B **62**, R6089 (2000)
50. M.A. Paalanen, J.E. Graebner, R.N. Bhatt, Phys. Rev. Lett. **61**, 597 (1988)
51. E. Bauer, St. Berger, Ch. Paul, M. Della Mea, G. Hilscher, H. Michor, M. Reissner, W. Steiner, A. Grytsiv, P. Rogl, E.W. Scheidt, Phys. Rev. B **66**, 214421 (2002)
52. T.H.K. Barron, J.G. Collins, G.K. White, Adv. Phys. **29**, 609 (1980)
53. O.V. Lounasmaa, in *Hyperfine Interactions*, edited by A.J. Freeman, R.B. Frenkel (Academic, New York, 1967), p. 467
54. H. Rudigier, H.R. Ott, O. Vogt, Phys. Rev. B **32**, 4584 (1985)
55. G.K. Shenoy, G.M. Kalvius, S.L. Ruby, B.D. Dunlap, M. Kuznietz, F.P. Campos, Int. J. Magn. **1**, 23 (1970)
56. A. Ishigaki, T. Mariya, J. Phys. Soc. Jpn **65**, 376 (1996)
57. C.V. Pandya, P.R. Vyas, T.C. Pandya, V.B. Gohel, Bull. Mater. Sci. **25**, 63 (2002)
58. D.M. Shermann, in *Physical Chemistry of Minerals and solutions*, (University of Bristol, England, 2005)
59. L. Zhu, M. Garst, A. Rosch, Quimiao Si, Phys. Rev. Lett. **91**, 066404 (2003)
60. R. Kuchler, N. Oeschler, P. Gegenwart, T. Cichorek, K. Neumaier, O. Tegus, C. Geibel, J.A. Mydosh, F. Steglich, L. Zhu, Q. Si, Phys. Rev. Lett. **91**, 066405 (2003)
61. D. Mandrus, B.C. Sales, V. Keppens, B.C. Chakoumakos, P. Dai, L.A. Boatner, R.K. Williams, J.R. Thompson, T.W. Darling, A. Migliori, M.B. Maple, D.A. Gajewski, E.J. Freeman, *Thermoelectric Materials - New Directions and Approaches. Symposium*, edited by T.M. Tritt, M.G. Kanatzidis, H.B. Jr. Lyon, G.D. Mahan, (Mater. Res. Soc. Pittsburgh, PA, USA, 1997) p. 197
62. J. Gan, E. Wong, Phys. Rev. Lett. **71**, 4226 (1993)
63. A.J. Millis, Phys. Rev. B **48**, 7183 (1993)
64. L. Qiu, M.A. White, Z. Li, J.S. Tse, C.I. Ratcliffe, C.A. Tulk, J. Dong, O.F. Sankey, Phys. Rev. B **64**, 024303 (2001)
65. L. Qiu, I.P. Swainson, G.S. Nolas, M.A. White, Phys. Rev. B **70**, 035208 (2004)
66. J.S. Tse, J. Phys. Colloq. France **48**, C1-543 (1987)
67. M. Zakrzewski, M.A. White, J. Phys.: Condens. Matter **3**, 6703 (1991)
68. A. Bentien, M. Christensen, J.D. Bryan, A. Sanchez, S. Paschen, F. Steglich, G.D. Stucky, B.B. Iversen, Phys. Rev. B **69**, 045107 (2004)
69. L. Girard, R. Viennois, L. Chapon, A. Haidoux, H. Mutka, J.-C. Tedenac, D. Ravot, *Proceedings ICT'03. 22nd International Conference on Thermoelectrics* (IEEE at Piscataway, NJ, USA), p. 72
70. J.L. Feldman, D.J. Singh, C. Kendziora, D. Mandrus, B.C. Sales, Phys. Rev. B **68**, 7410 (1999)
71. A.B. Kaiser, AIP Conference Proceedings **29**, 364 (1976)
72. K. Fischer, J. Low Temp. Phys. **17**, 87 (1974)
73. T. Takegahara, H. Harima, J. Phys. Soc. Jpn. **69**, 2938 (2000)